International Journal of Advanced Science and Technology
Vol.88 (2016), pp.43-62
http://dx.doi.org/10.14257/ijast.2016.88.05

Opposing and Assisting Flow Characteristics of Radiative Casson Fluid due to Cone in the Presence of Induced Magnetic Field

C. S. K. Raju[1] and N. Sandeep[2*]

[1,2] *Department of Mathematics, VIT University, Vellore-632014, India*
[1]*sivaphd90@gmail.com*, [2]*dr.nsrh@gmail.com*

Abstract

In this study, we investigated the induced magnetic field and nonlinear thermal radiation effects on Casson fluid flow over a cone in the presence of chemical reaction. The coupled non-linear transformed governing equations are solved numerically using Runge-Kutta based shooting technique. We obtain good accuracy of the new results by comparing with the published results. In this study we presented dual solutions for opposing and assisting flows over a cone. The influence of dimensionless parameters on velocity, temperature and concentration profiles along with the friction factor coefficient, local Nusselt and Sherwood numbers are discussed with the help of graphs and tables. It is observed that the effect of induced magnetic field is highly significant while controlling the flow field.

Keywords**:** *Induced magnetic field, nonlinear thermal radiation, chemical reaction, Casson fluid, assisting and opposing flows*

1. Introduction

The Casson fluid is a familiar with a rheological fluid model for describing the non-Newtonian fluid flow properties with yield stresses. This model was originated due to viscous suspension of cylindrical particles in a flow. Despite of few fluids are described well due to their nonlinearity and yielding stresses in the flow are pseudo plastic in nature. For example waxy crude oil, slurries, blood, chocolate, waste water sludge's and gum solutions. Casson model is a special case of power-law model and it has benefitted in many industrial processes such as aerospace technology, pharmaceutical engineering industries, food processing technology, various hospital treatments and polymer production. In view of these studies [1-4] are starting the research on Casson fluid model. Kelessidis and Maglione [5] the rheological Casson model characteristics of betonies suspensions and true shear rates in coquette Viscometer. An unsteady MHD convection flow over an impulsively vertical permeable plate in the presence of radiation was investigated by Sandeep [6]. Shehzad *et al.*, [7] discussed the radiation effect on Jeffery fluid flow past a stretching sheet in the presence of thermophoresis and joule heating effects. The non-Newtonian fluid flow characteristics of MHD flow past a permeable exponentially stretching surface was examined numerically by Raju *et al.*, [8]. Mahantesh *et al.*, [9] analyzed the non-uniform heat source/sink effect on Walter's Liquid B fluid flow over an impermeable stretching sheet. Hayat *et al.*, [10] considered the convective conditions on three-dimensional Oldroyd-B fluid flow over a stretching surface.

The recent development of modern technologies has stimulated excitement in fluid flows past a cone. It has profited applications in many of the real life industrial, healthcare safety management systems and engineering applications like preparation of transmission missile gun operations, aeronautical engineering, hydrology, geosciences, development of electronic chips, solar collectors, scanning, Homeo-therapy treatment, endoscopy scanning, radiology treatment, nuclear safety and cleaning management systems, dental applications, astrophysics, paper production industries, lubricating grease for seals,

ISSN: 2005-4238 IJAST

valves, and threaded connections. Flow over a cone with radiation also plays an important role in many of science, medical and engineering processes like petroleum industries, pharmaceutical chemistry, inverting solar pumps, environmental controlling and plantation. Due to this importance the Hering and Grosh [11] started the convection flow over rotating cone. Anilkumar and Roy [12] illustrated an unsteady flow on a rotating cone in the presence of rotating fluid. Nadeem and Saleem [13] investigated an unsteady convection flow on rotating frame in the presence of magnetic field effects. Raju *et al.*, [14] studied the radiation effect on Jeffrey nanofluid flow past a cone in the presence of chemical reaction parameter and magnetic field effect. In this paper they concluded that the momentum boundary layer is controlled by the mixed convection parameter. The analytical treatment of non-Newtonian nanofluid flow over a rotating cone with the rotation effect was investigated by Nadeem and Saleem [15]. Ahmad *et al.*, [16] discussed the opposing and assisting flow characteristics of boundary layer flow along thin vertical needles. Mixed convection flow past a vertical permeable surface in the presence of buoyancy forces was considered by Subhashini *et al.*, [17]. Jayachandrababu *et al.*, [18] examined the Brownian motion and thermophoresis effects on Eyring-Powell nanofluid past a permeable cone in the presence of magnetic field and concluded that magnetic field effect controls the flow.

Heat and mass transfer in the flow over a cone with chemical reaction parameter has a major role in chemical engineering industries and metallurgy such as polymer production and food processing. Moreover, it also has a more important in many processes such as drying, evaporation at the surface of a water body and energy transfer in a wet cooling tower, preparation of pure water solutions, damage of crops due to freezing, distribution of temperature and moisture over agricultural fields, groves of fruit trees, dispersion of chemical from the water, synthesis of chemical bond removing pollutant chemicals, etc. Due to this the influence of chemical reaction on the flow past various channels were discussed by the researchers [19-22]. Ishak *et al.*, [23] analyzed the micropolar fluid flow of stagnation point flow towards a stretching surface and highlight the stretching ratio parameter suppresses the thermal boundary thickness for both the opposing and assisting flow cases. The induced magnetic field contains a both the mechanical and electrical properties, which describes the motion of highly conducting fluid with existing of magnetic field. The main advantage of the induced magnetic field is to convert the mechanical energy into electrical energy. The induced magnetic field is also major applications in the psychological fluids like a peristaltic MHD compressor, blood pumping machines and the blood flows, MHD accelerators, Generators, pumps and flow meters, design of cooling systems, meteorology engineering, cosmetic fluid mechanics, geophysics, nuclear reactors, power generation spacecraft, wind tunnel applications, magneto hydrodynamic laser power generators, uninterrupted power plants systems, electric power production system etc. The researchers Hayat *et al.*, [24], Jayachandrababu *et al.*, [25], Ali *et al.*, [26] discussed the induced magnetic field effect on the flow through different channels. Sandeep and Sulochana [27] presented dual solutions for unsteady mixed convection flow of MHD micropolar fluid over a stretching/shrinking sheet. The reachers [28-30] discussed heat and mass transfer in some MHD flows by considering different channels.

Motivations of above studies, the present paper address the induced magnetic field and nonlinear thermal radiation effects on Casson fluid flow over a cone in the presence of chemical reaction. The transformed governing equations are solved numerically using Runge-Kutta based shooting technique. The influence of dimensionless parameters on velocity, temperature and concentration profiles along with the friction factor, local Nusselt and Sherwood numbers are discussed with the help of graphs and tables.

2. Formulation of the Problem

Consider a steady two-dimensional flow of Casson fluid over a cone in the presence of chemical reaction and non-linear thermal radiation. An induced magnetic field of strength B_0 is applied along z -direction, which is normal to the cone. It is assumed that the applied magnetic field is of uniform strength B_0 . Here the parallel component B_1 approaches the value $B_e = B_0$ in the free stream flow and normal component of the induced magnetic field B_2 vanishes near the wall. T_w and T_∞ are indicates the temperatures near and far away from the surface.

2.1. Flow Analysis:

$$\frac{\partial}{\partial x}(ru) + \frac{\partial}{\partial y}(rv) = 0, \tag{1}$$

$$\frac{\partial rB_1}{\partial x} + \frac{\partial rB_2}{\partial y} = 0, \tag{2}$$

$$\left(u\frac{\partial u}{\partial x} + v\frac{\partial u}{\partial y} - \frac{\mu}{4\pi\rho}\left(B_1\frac{\partial B_1}{\partial x} + B_2\frac{\partial B_1}{\partial y}\right)\right) = \left(v\left(1+\frac{1}{\beta}\right)\frac{\partial^2 u}{\partial y^2} + u_e\frac{du_e}{dx} - \frac{\mu B_e}{4\pi\rho}\frac{dB_e}{dx}\right) \pm g\beta_T(T-T_\infty)\cos\gamma \pm g\beta_c(C-C_\infty)\cos\gamma, \tag{3}$$

$$\left(u\frac{\partial B_1}{\partial x} + v\frac{\partial B_1}{\partial y} - B_1\frac{\partial u}{\partial x} - B_2\frac{\partial u}{\partial y}\right) = \mu_e\frac{\partial^2 B_1}{\partial y^2}, \tag{4}$$

with the boundary conditions

$$\left.\begin{aligned} &u = u_w(x) = c(v/x)(Gr)^{1/2}, v = 0, \frac{\partial B_1}{\partial y} = B_2 = 0, \qquad \text{at } y = 0, \\ &u = u_e(x) = a(v/x)(Gr)^{1/2}, \frac{\partial u}{\partial y} \to 0, \frac{\partial v}{\partial y} \to 0, B_1 = B_e(x) = B_0(v/x)(Gr)^{1/2}, \quad \text{as } y \to \infty, \end{aligned}\right\} \tag{5}$$

μ_e is the magnetic diffusivity of the fluid, which is given by $\mu_e = \frac{1}{4\pi\sigma}$, (6)

where u, v are the velocity components along the x, y directions respectively. β is the Casson fluid parameter, B_1, B_2 are the induced magnetic components in x and y directions. B_0 is the induced magnetic component in free stream flow, B_e is the induced component at the edge, u_e is the velocity component at the edge, g is the acceleration due to gravity, a, c are the constant velocities, ν is the kinematic viscosity coefficient,. To convert the nonlinear partial differential equations for velocities, we now introducing the self-similarity transformations are given by:

$$\left.\begin{aligned} &u = \frac{cv_f}{x}(Gr)^{1/2} f'(\eta), v = \frac{cv_f}{x}(Gr)^{1/4}\left(\frac{\eta}{4}f'(\eta) - \frac{1}{2}f(\eta)\right), \eta = \frac{y}{cx}(Gr)^{1/4}, \\ &B_1 = \frac{B_0}{x}(Gr)^{1/2} G'(\eta), B_2 = \frac{B_0}{x}(Gr)^{1/4}\left(\frac{\eta}{4}G'(\eta) - \frac{1}{2}G(\eta)\right), T = T_\infty + (T_w - T_\infty)\theta(\eta) \\ &Gr = \frac{\rho g x^3 \beta_T \cos\Omega (T_w - T_\infty)}{\nu^2}, C = C_\infty + (C_w - C_\infty)\phi(\eta) \end{aligned}\right\} \tag{7}$$

Here in equation (7) u, v and B_1, B_2 are automatically satisfy the continuity equation, by using equation (7), the equations (1) to (3) transformed equations are given by:

$$\left(1+\frac{1}{\beta}\right) f'''+ ff''-\frac{f'^2}{2}+\frac{1}{2} ff''+\frac{a^2}{c^2}+\frac{M}{2}(G'^2-GG''-1)\pm\lambda\phi\pm\theta=0, \tag{8}$$

$$\varepsilon G'''+\frac{fG''}{2}-\frac{f''G}{2}=0, \tag{9}$$

The transformed boundary conditions are:

$$\left.\begin{array}{ll} f=0, g=0, f'=1, g''=0, & at\ \ \eta=0, \\ f'\to a/c, g'\to 1, & as\ \ \eta\to\infty, \end{array}\right\} \tag{10}$$

here M is the magnetic field parameter, λ is the buoyancy parameter, β is the Casson fluid parameter, ε and is the magnetic prandtl number, $\lambda\succ 0$ is for assisting flow and $\lambda\prec 0$ is for opposing flow.

$$\left.M=\frac{\mu_f B_0^2}{4\pi\rho_f c^2}, \varepsilon=\frac{1}{4\pi\sigma_f \upsilon_f}, \lambda=\frac{\beta_C (C_w-C_\infty)}{\beta_T (T_w-T_\infty)}\right\} \tag{11}$$

2.2. Heat Transfer Analysis:

The boundary layer thermal energy equation with nonlinear thermal radiation is given by

$$u\frac{\partial T}{\partial x}+v\frac{\partial T}{\partial y}=\alpha\frac{\partial^2 T}{\partial y^2}+\frac{16\sigma^*}{3k\rho c_p}\frac{\partial T}{\partial y}\left(T^3\frac{\partial T}{\partial y}\right), \tag{12}$$

With the corresponding boundary conditions are

$$T=T_w,\ \text{at}\ y=0,\ T\to T_\infty,\ \text{as}\ \ y\to\infty, \tag{13}$$

The non-dimensional temperature is given by

$$T=T_\infty+(T_w-T_\infty)\theta, T=T_\infty(1+(\theta_w-1)\theta) \tag{14}$$

where T is the fluid temperature, T_w, T_∞ are the near the fluid temperature and the far away from the fluid temperature, k is the thermal conductivity of the fluid, c_p is the specific heat capacitance at constant pressure, c_s is the concentration susceptibility and σ^* is the Stefan-Boltzmann constant.

By using self-similarity transformations of (13), (14), equation (12) reduced to

$$\theta''+\frac{\Pr}{2} f\theta'+R\left(\left(1+(\theta_w-1)\theta\right)^3\theta''+3(\theta_w-1)\theta'^2\left(1+(\theta_w-1)\theta\right)^2\right)=0, \tag{15}$$

With the transformed boundary conditions

$$\theta(0)=1,\ \theta(\infty)=0, \tag{16}$$

Where $\Pr$ is the Prandtl number, R is the thermal radiation parameter, θ_w is the ratio of temperatures which are given by

$$\Pr=\frac{k}{\mu C_p}, R=\frac{16\sigma^* T_\infty^3}{3kk^*}, \theta_w=\frac{T_\infty}{T_w}, \tag{17}$$

2.3. Mass Transfer Analysis:

The boundary layer equation of mass diffusion equation in the presence of chemical reactions is given by

$$u\frac{\partial C}{\partial x}+v\frac{\partial C}{\partial x}=D_m\frac{\partial^2 C}{\partial y^2}-k_l(C-C_\infty), \tag{18}$$

The corresponding boundary conditions are

$$C=C_w \ at \ \ y=0,\ C\to C_\infty, \quad as \quad y\to\infty, \tag{19}$$

Where D_m are the diffusion coefficient, k_l is the chemical reaction parameter,

$$\frac{1}{Sc}\phi''+\frac{1}{2}f\phi'-\phi Kr=0, \tag{20}$$

The corresponding boundary conditions are

$$\phi=1, at \ \ \eta=0, \phi=0, \ as \ \ \eta\to\infty, \tag{21}$$

Where Sc is the Schmidt number, Kr is the chemical reaction parameter, which are given by

$$Sc=\frac{\nu}{D_A}, Kr=\frac{k_l x^2}{\nu(Gr)^{1/2}}, \tag{22}$$

For physical quantities of interest the friction factor coefficients, local Nusselt and Sherwood numbers are given by

$$C_{fx}\,\mathrm{Re}^{1/2}=\left(1+\frac{1}{\beta}\right)f''(0), \tag{23}$$

$$\mathrm{Re}^{-1/2}\,Nu_x=-\theta'(0), \mathrm{Re}^{-1/2}\,Sh_x=-\phi'(0). \tag{24}$$

Where $\mathrm{Re}=\frac{xu_w(x)}{\nu}$ is the Reynolds number.

3. Results and Discussion

The set of nonlinear coupled ordinary differential equations (8), (9), (15) and (20) subjected to the boundary conditions (10), (16) and (21) are solved numerically using Runge-Kutta based shooting method (Sandeep and Sulochana [27]). Results shows the influence of non-dimensional governing parameters on velocity, temperature and concentration profiles along with the friction factor coefficient, local Nusselt and Sherwood numbers. For numerical computations we considered the non-dimensional parameter values as $\varepsilon=5, \lambda=0.1, a/c=0.5, \beta=0.2, Kr=0.3, R=5, \theta_w=1.1, Sc=0.6, \mathrm{Pr}=6.2$. These values are kept as common in entire study except the variations in respective figures and tables. In graphical results red color indicates the assisting fluid flow over a cone while green color indicates the opposing fluid flow over a cone.

The effect of magnetic field parameter on velocity fields for both the assisting and opposing flow over a cone are displayed in Figures 1 and 2. Which shows that the velocity and induced velocity profiles are decreased with an improved values of magnetic field parameter when $a/c<1$. Whereas the velocity, induced velocity profiles are enhanced with magnetic field parameter when $a/c>1$. These are displayed in Figures 3 and 4. Physically, increasing values of magnetic field parameter creates a drag force opposite to the flow direction. Also the buoyancy forces are highly influenced near the cone. The drag force and buoyancy forces dominates the induced profiles. Due to this forces the velocity, induced velocity profiles are depreciated when $a/c<1$. From

Figures 5-8 it clear that increasing values of a/c enhances the velocity and temperature for both the assisting and opposing flows. But reverse results have been observed for induced velocity and concentration profiles. Fundamentally, improved values of a/c improves the straining motion near the cone this can leads to enhancing the acceleration of the external stream of cone. Due to this reason the velocity and temperature fields are enhanced. The effect of chemical reaction parameters on the concentration profiles are plotted in Figure 9 for both opposing and assisting flows. Increasing values of chemical reaction parameter fall down in the concentration profiles for both cases. Physically, deviation in the chemical reaction parameter fluctuate the diffusivity of the flow and creates a local buoyancy forces. This may be cause to reduce the concentration profiles.

Figures 10-13 display the influence of buoyancy parameter on velocity, induced velocity, temperature and concentration profiles of the flow for both the opposing and assisting flows over a cone. It noticed that the velocity, induced velocity and temperature fields are improved in assisting flow over a cone, whereas the concentration profiles are depreciated. The opposite results are observed in opposing flow over a cone. These may be due to the fact that in opposing flow buoyancy forces are working on opposite direction, due to this reason we saw a decrement in velocity, induced velocity and temperature profiles of the flow.

The velocity, induced velocity, temperature and concentration distributions for various values of Casson fluid parameter β for both assisting and opposing flow over cone are observed in Figures 14-17. The dual behavior was observed in Casson fluid parameter. The casson fluid parameter boost up the velocity, induced velocity and temperature profiles of the flow for assisting flow over cone. But exactly opposite phenomena was observed in opposing flow over a cone. We have seen reverse results to above for concentration profiles. Figures 18-20 show the effect of radiation parameter on velocity, induced velocity and temperature profiles for both assisting and opposing flows over a cone. Basically, the larger values of radiation parameter produce more heat working on the fluid that appears an enhancement in the temperature profiles. Table 1 demonstrates the comparison of the present results with the existed literature under some limited cases. We found better agreement of the present results with the published literature. This proves the validity of the obtained results along with the accuracy of the numerical technique we used in the present study.

Tables 2 and 3 illustrate the variations in the friction factor coefficients, local Nusselt and the Sherwood numbers for both the assisting and opposing flows over a cone with different values of non-dimensional governing parameters. It is observed that rise in the values of a/c improves the fiction factor coefficients as well as Sherwood number and reduces the Nusselt number values for both assisting and opposing fluid flows over a cone. The Sherwood number is boost up in the presence of chemical reaction parameter for both cases. The heat transfer rate is improved for higher values of radiation parameter. It is interesting to mention that the radiation parameter enhances the friction factor, mass transfer rate in opposing flow over a cone and depreciates the assisting flow over a cone. The Casson fluid parameter encourages the heat transfer rate, friction factor coefficients and depreciates the mass transfer rate in opposing flow over a cone. Whereas the friction factor coefficient, Sherwood numbers are hike in the assisting fluid flow over a cone and suppresses the heat transfer rate. The magneticfield is help to improve the Nusselt number and reduces the friction factor coefficient, Sherwood numbers for both assisting and opposing flows over a cone. The friction factor coefficient, Sherwood numbers are depreciated and the Nusselt number is enhanced with an increasing values of buoyancy parameter in opposing fluid flow over a cone. The exactly opposite phenomenon has been observed in assisting flow over a cone.

Table 1. Validation of Friction Factor Coefficient and Nusselt Number when $\lambda = Kr = R = \theta_w = Sc = 0,\ \beta \to \infty, \varepsilon = 5, \Pr = 0.72.$

	$a/c = 3$					$a/c = 0.5$			
M	Ali et al. [26]	Ali et al. [26]	Present	Present	M	Ali et al. [26]	Ali et al. [26]	Present	Present
0.1	4.70928	0.97902	4.70927	0.97902	0.1	-0.57595	0.59171	-0.57595	0.59171
0.5	4.62764	0.97617	4.62765	0.97617	0.15	-0.50938	0.60207	-0.50938	0.60207
1	4.52158	0.97240	4.52158	0.97240	0.2	-0.40717	0.61811	-0.40717	0.61811
2	4.29431	0.96405	4.29431	0.96405	--	--	--	--	--
5	3.43352	0.92863	3.43352	0.92863	--	--	--	--	--
8	1.87734	0.84494	1.87732	0.84493	--	--	--	--	--

Table 2. The Physical Parameter Values of Skin Friction Coefficient, Local Nusselt and Sherwood Numbers for Opposing Flow over a Cone

M	Kr	λ	β	R	a/c	$f''(0)$	$-\theta'(0)$	$-\phi'(0)$
0.1						-0.644567	0.130712	0.487019
0.3						-0.656029	0.131213	0.485955
0.5						-0.666683	0.131656	0.484992
	0.1					-0.699707	0.110696	0.357349
	0.3					-0.695720	0.110382	0.476268
	0.5					-0.693024	0.110181	0.575248
		0.1				-0.643928	0.130684	0.487079
		0.3				-0.693515	0.132380	0.483378
		0.5				-0.744655	0.134197	0.479442
			0.01			-5.015035	0.086249	0.519893
			0.03			-4.704197	0.087783	0.517279
			0.04			-4.468622	0.089223	0.514801
				0.4		-3.488740	0.002178	0.463328
				0.8		-3.338837	0.015574	0.468776
				1.2		-3.229406	0.031528	0.472608
					0.2	-3.839582	0.128894	0.446672
					0.4	-3.239869	0.115308	0.468583
					0.6	-2.789320	0.105643	0.483553

Table 3. The Physical Parameter Values of Skin Friction Coefficient, Local Nusselt and Sherwood Numbers for Assisting Flow over a Cone

M	Kr	λ	β	R	a/c	$f''(0)$	$-\theta'(0)$	$-\phi'(0)$
0.1						0.134106	0.099339	0.549923
0.3						0.101103	0.100892	0.547176
0.5						0.067343	0.102481	0.544338
	0.1					0.166999	0.067084	0.467148
	0.3					0.165788	0.067130	0.553500
	0.5					0.164766	0.067166	0.633649
		0.1				0.135865	0.099257	0.550068
		0.3				0.173597	0.098481	0.551929
		0.5				0.210980	0.097726	0.553751
			0.01			-0.030241	0.072833	0.542008
			0.03			0.174674	0.072311	0.542929
			0.04			0.313761	0.071839	0.543775
				0.4		0.899177	0.003284	0.557767
				0.8		0.837191	0.017151	0.556200
				1.2		0.772856	0.035569	0.554602
					0.2	0.235704	0.075338	0.542499
					0.4	0.553536	0.069812	0.549886
					0.6	0.892147	0.064446	0.5571

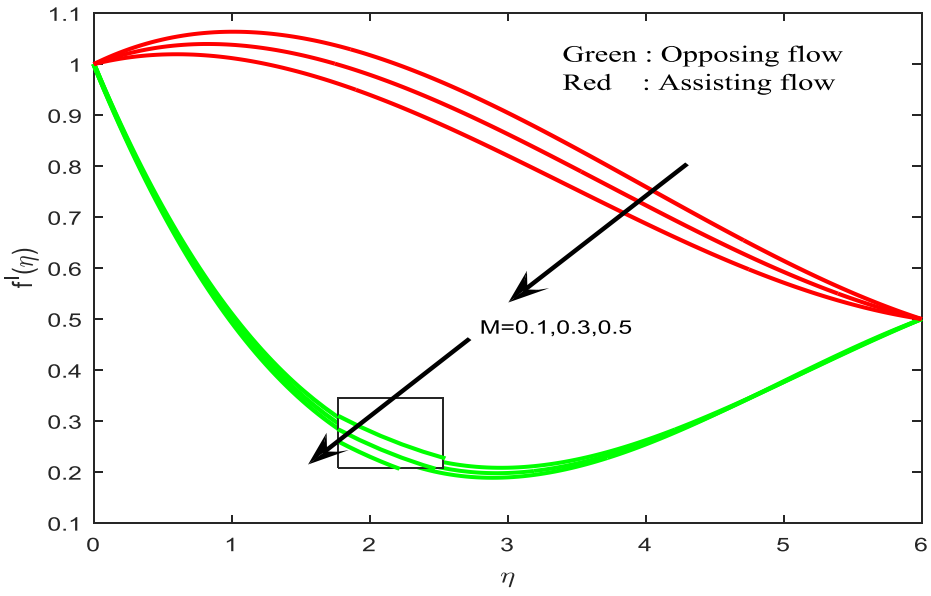

Figure 1. Velocity Profile for Different Values of Magneticfield Parameter when $a/c = 0.5$

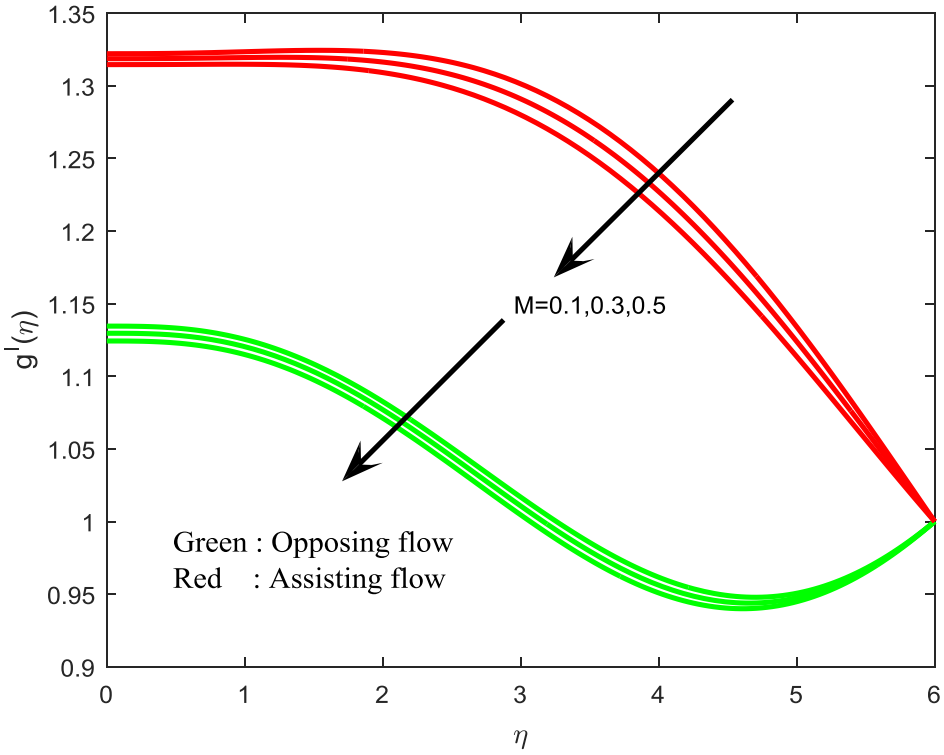

Figure 2. Induced Velocity Profiles for Different Values of Magneticfield Parameter when $a / c = 0.5$

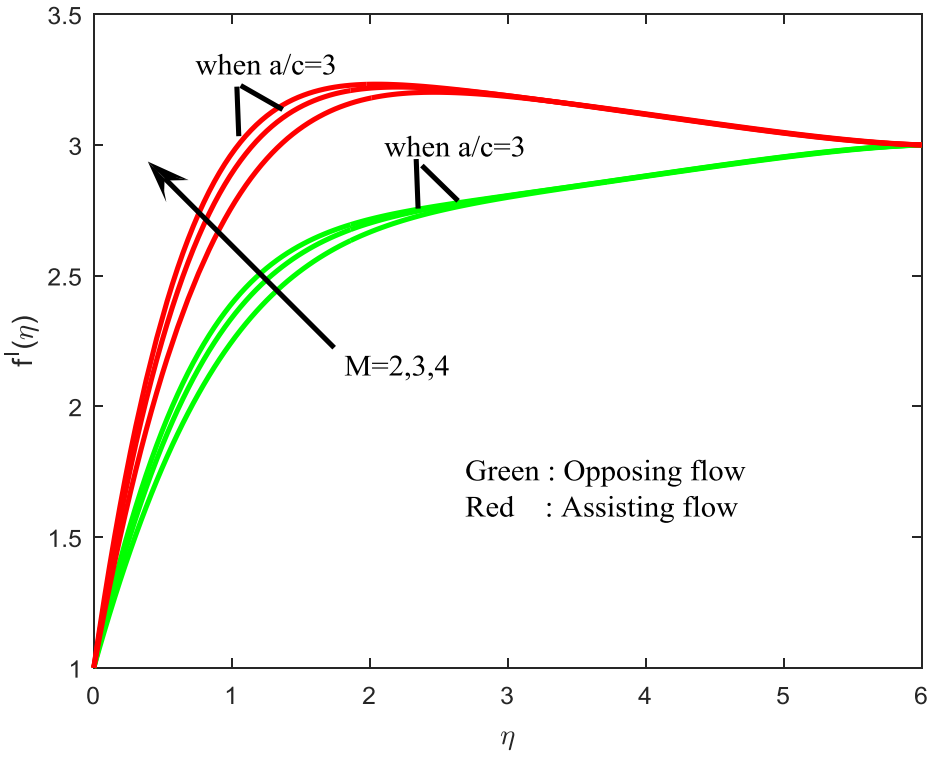

Figure 3. Velocity Profiles for Different Values of the Magneticfield Parameter

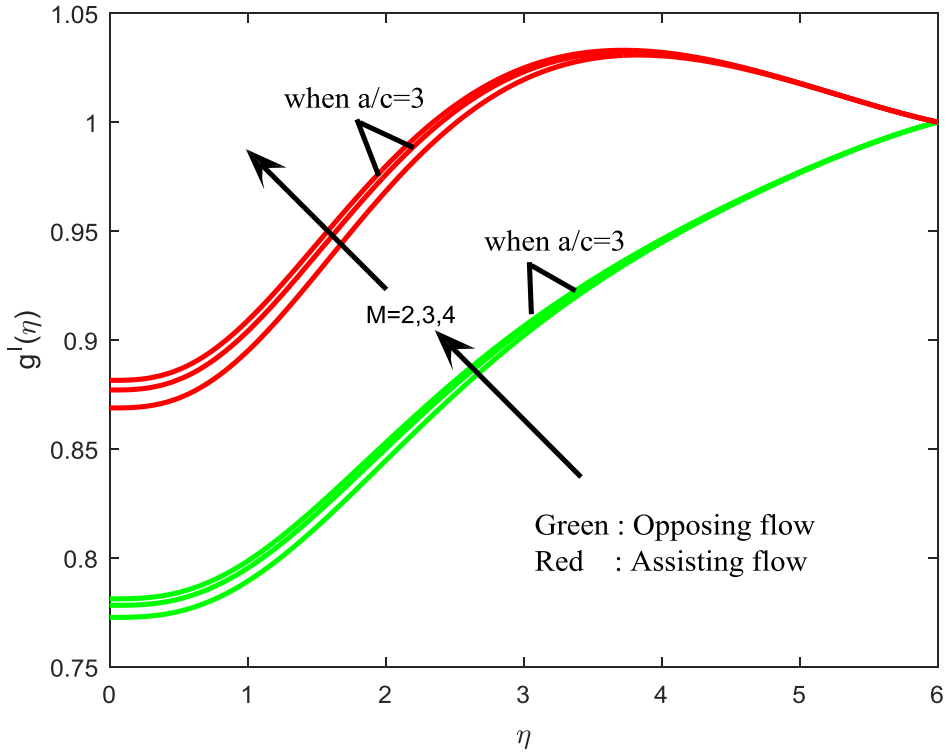

Figure 4. Induced Velocity Profiles for Different Values of the Magneticfield Parameter

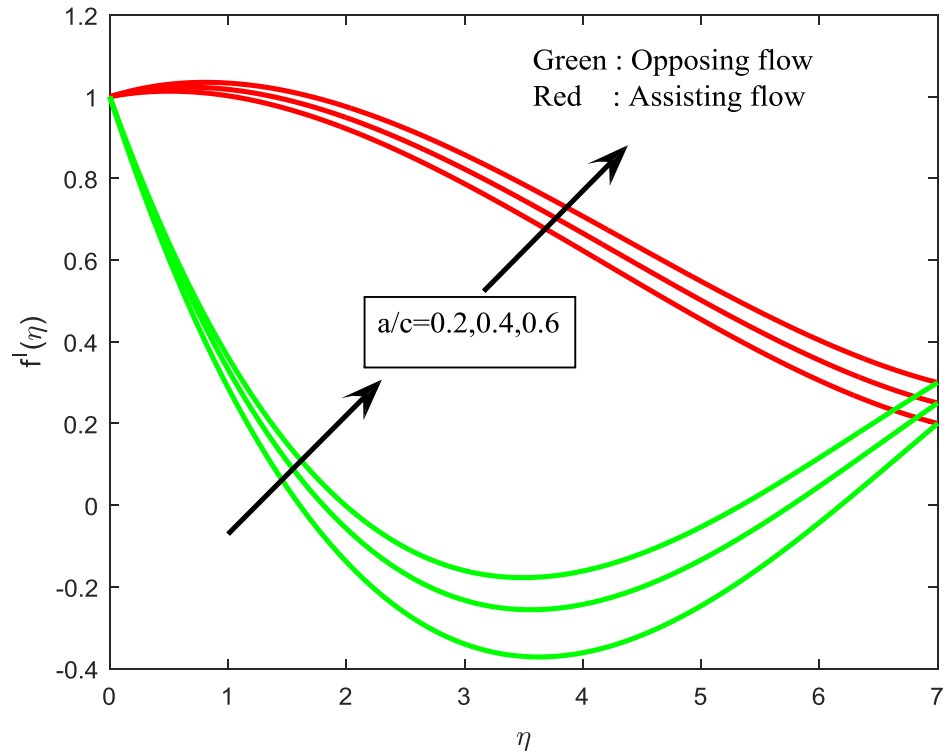

Figure 5. Velocity Profiles for Different Values of the a / c

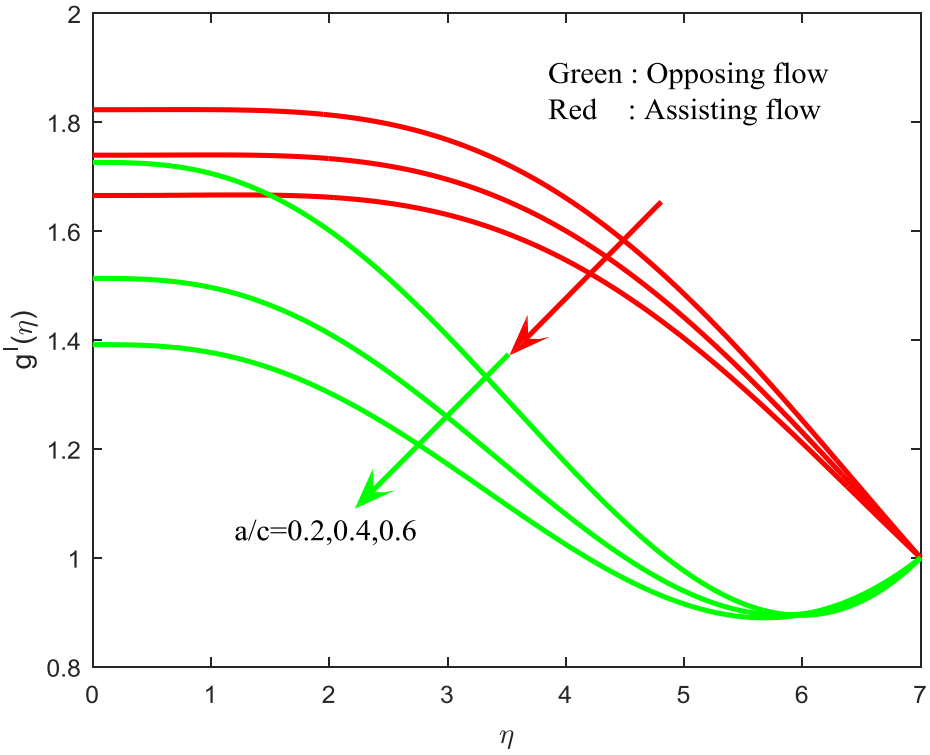

Figure 6. Induced Velocity Profile for Different Values of the a / c

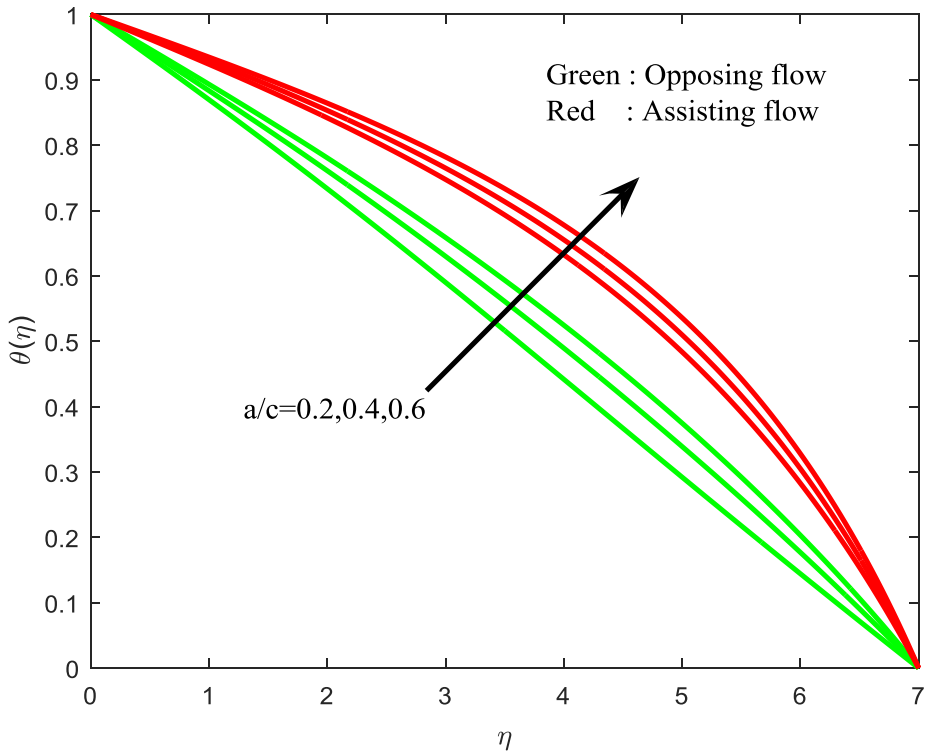

Figure 7. Temperature Profiles for Different Values of a / c

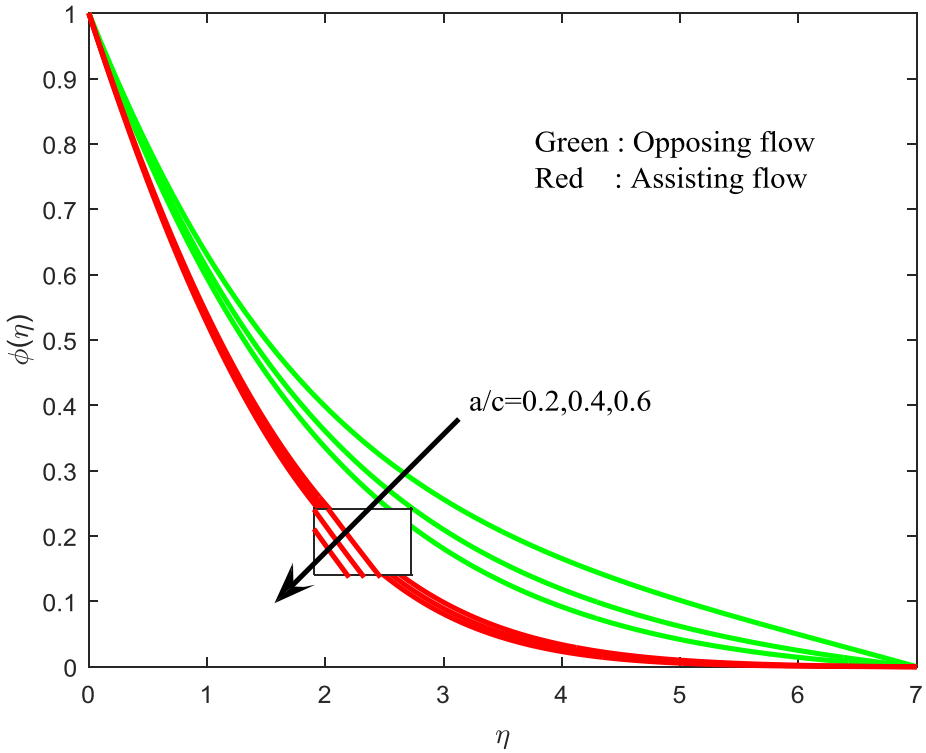

Figure 8. Concentration Profiles for Different Values of a / c

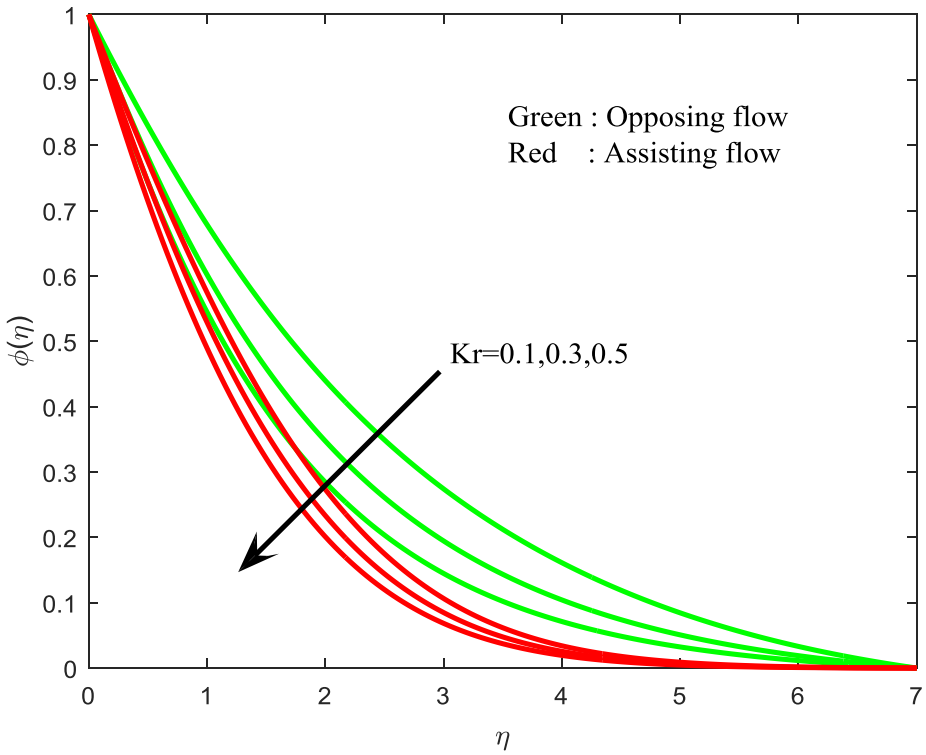

Figure 9. Concentration Profiles for Different Values of Chemical Reaction Parameter

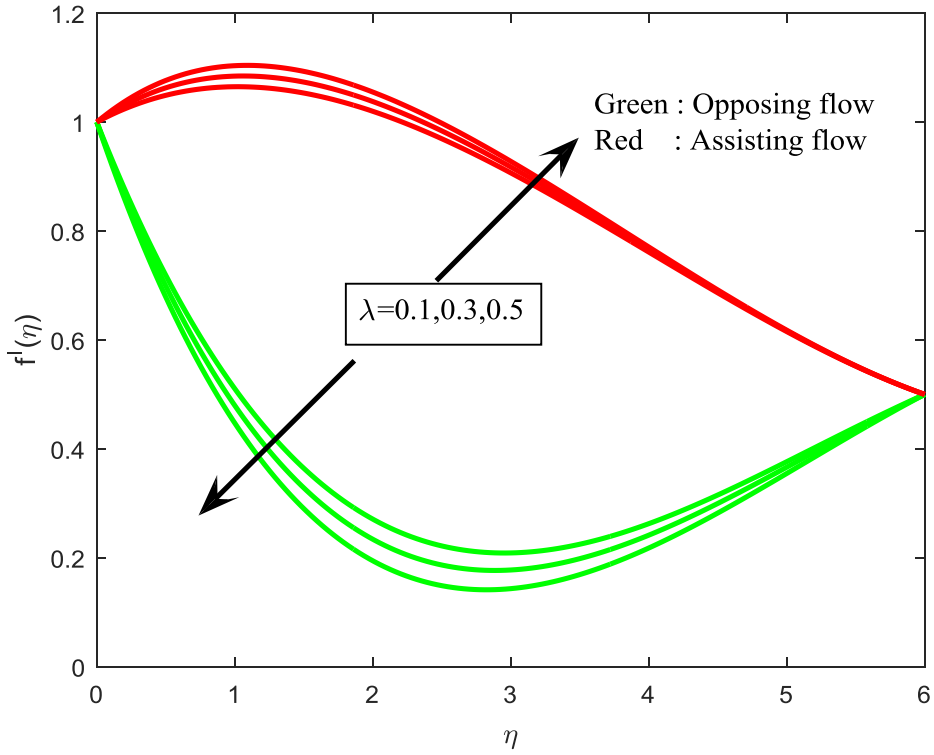

Figure 10. Velocity Profiles for Different Values of Buoyancy Parameter

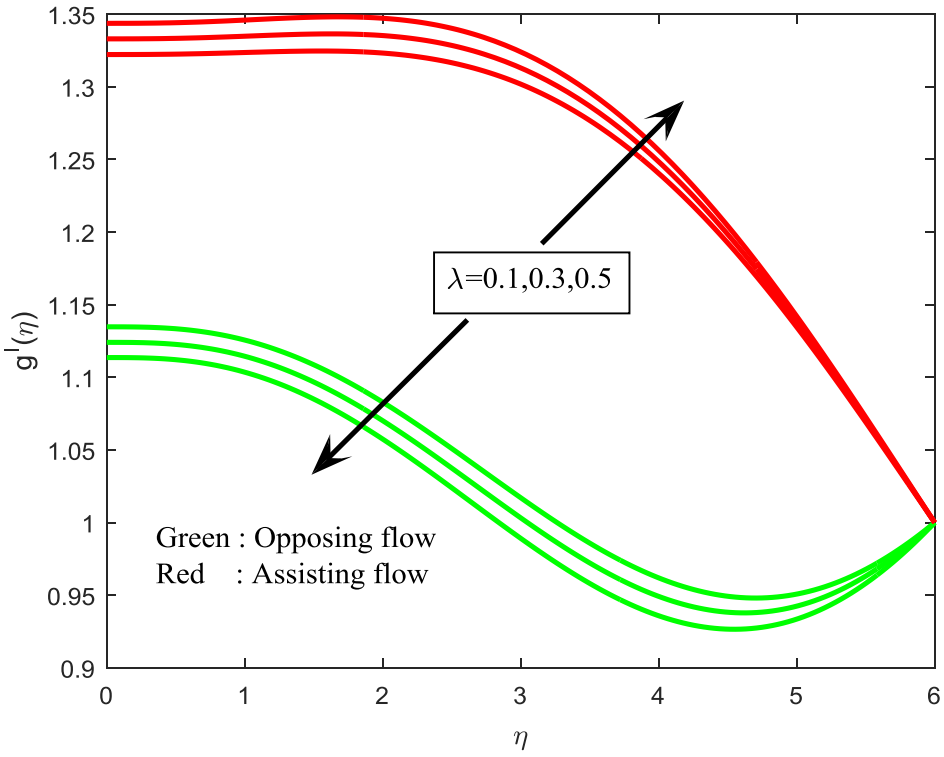

Figure 11. Induced Velocity Profiles for Different Values of Buoyancy Parameter

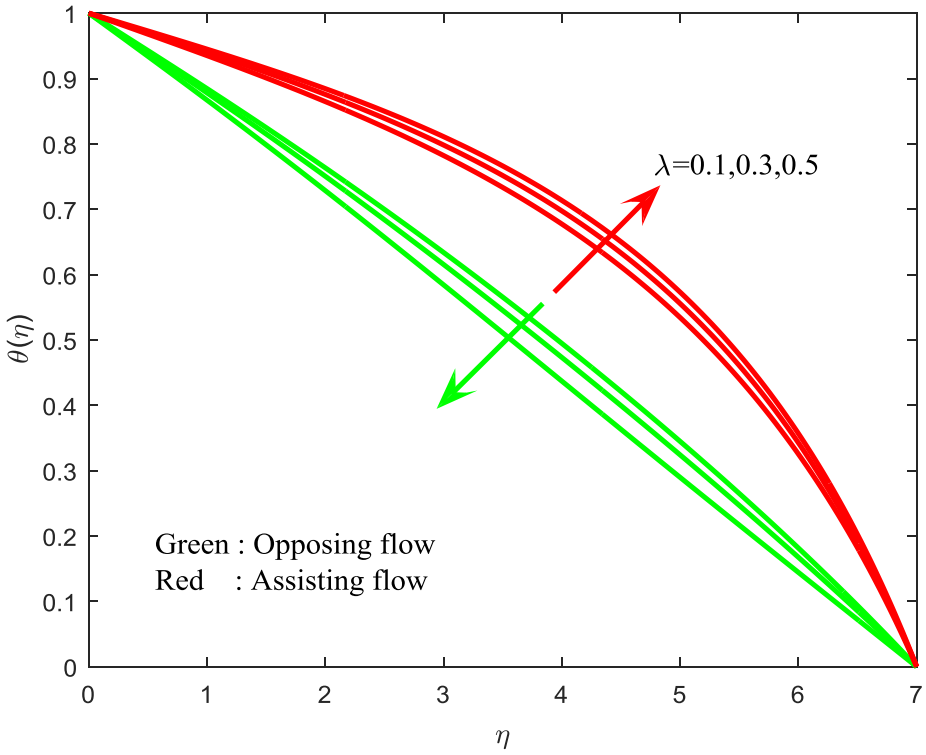

Figure 12. Temperature Profiles for Different Values of Buoyancy Parameter

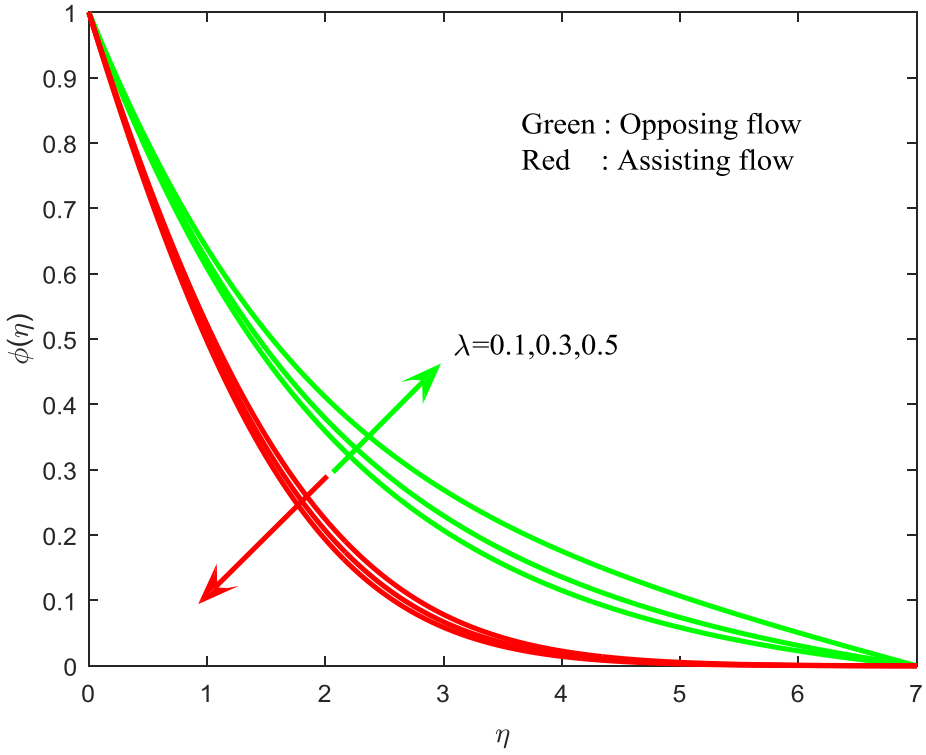

Figure 13. Concentration Profiles for Different Values of Buoyancy Parameter

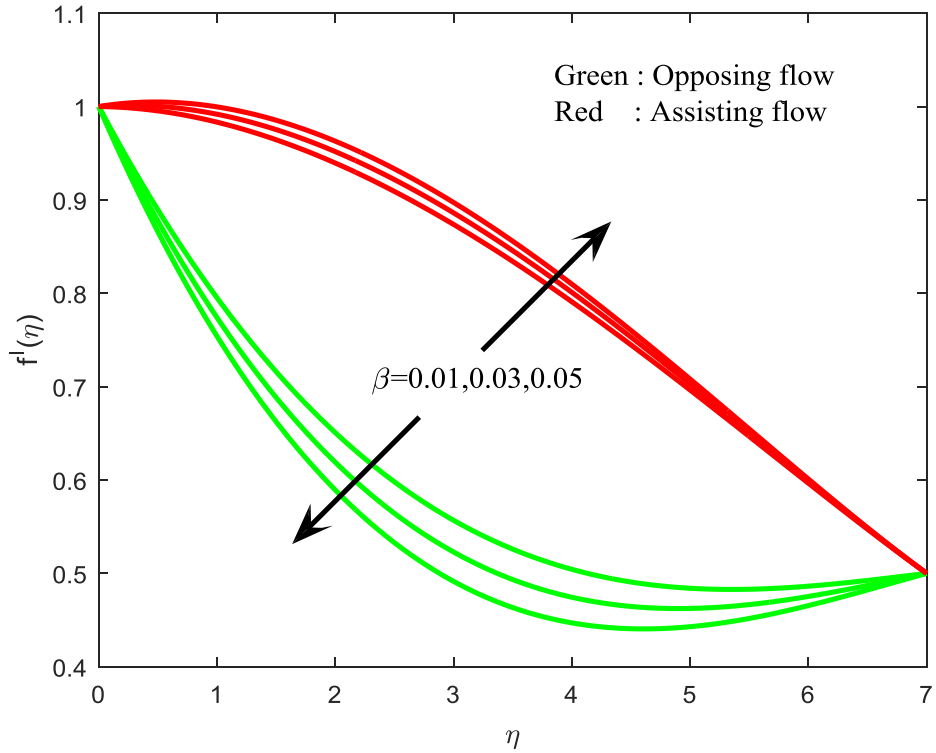

Figure 14. Velocity Profiles for Different Values of Casson Fluid Parameter

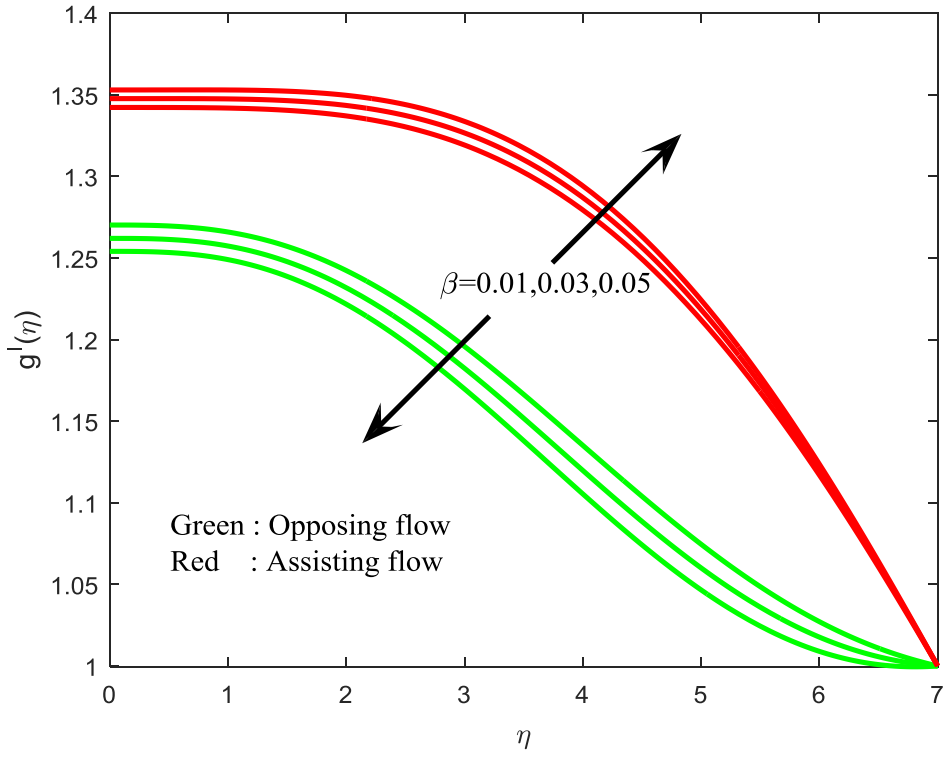

Figure 15. Induced Velocity Profiles for Different Values of Casson Fluid Parameter

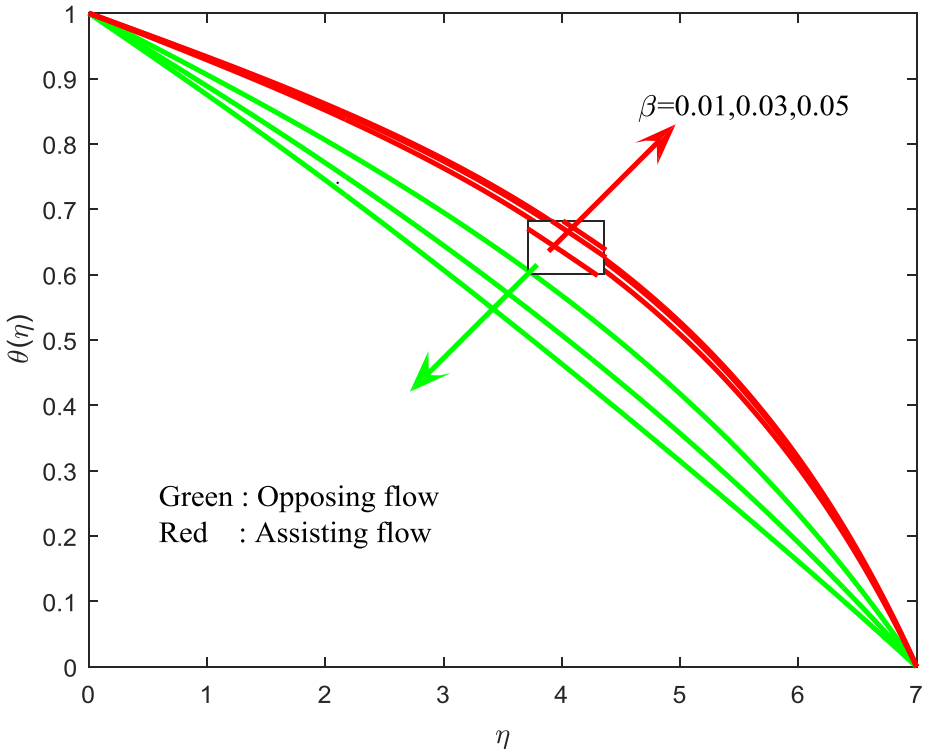

Figure 16. Temperature Profiles for Different Values of Casson Fluid Parameter

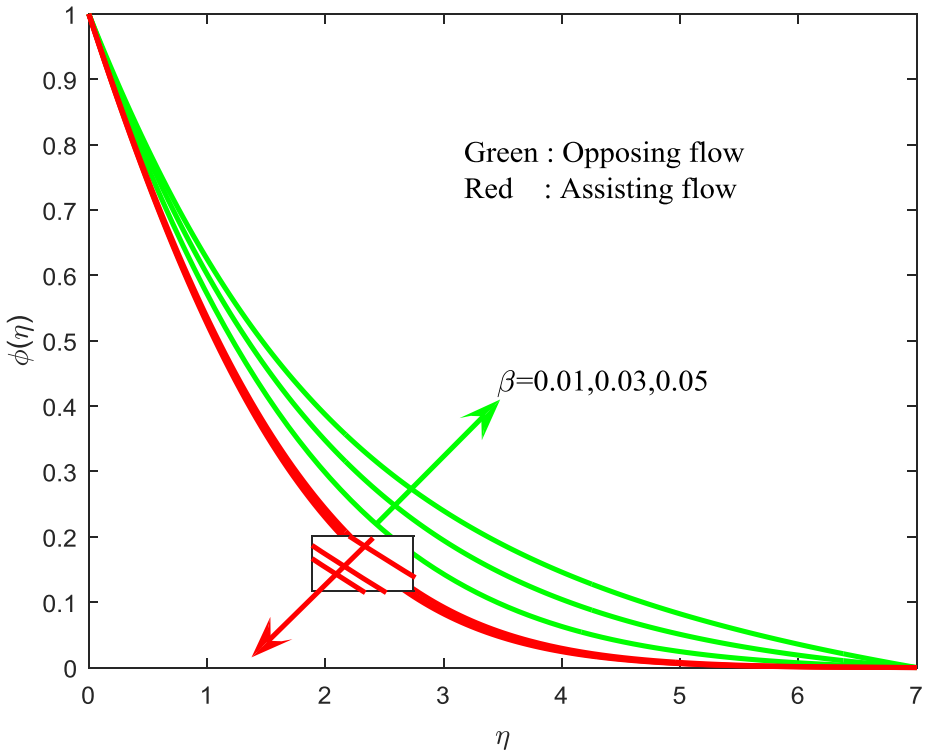

Figure 17. Concentration Profiles for Different Values of Casson Fluid Parameter

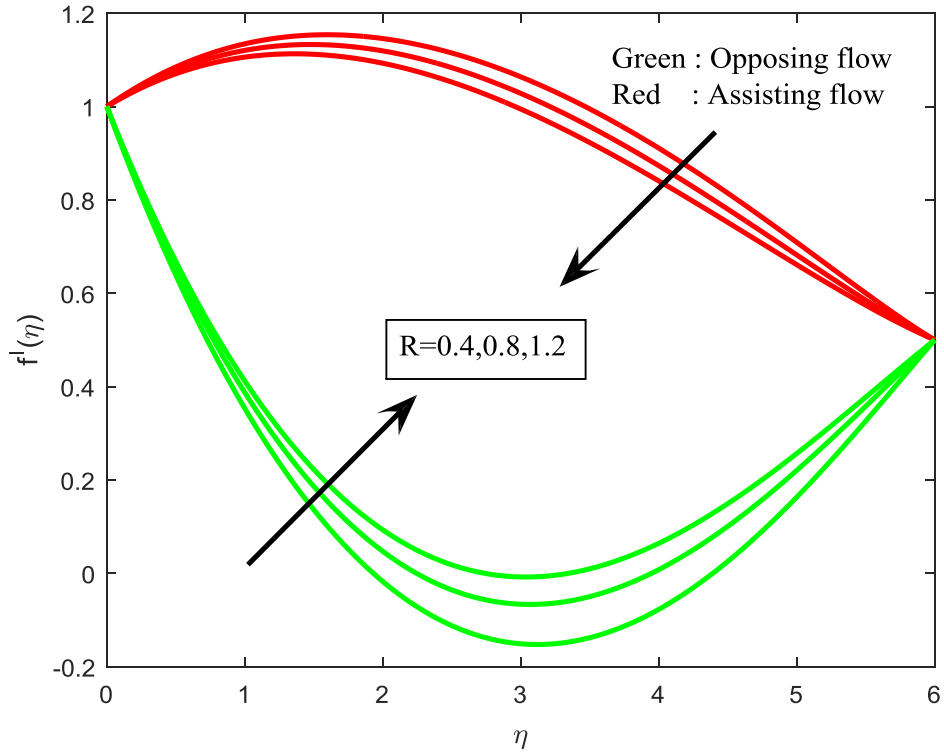

Figure 18. Velocity Profiles for Different Values of Radiation Parameter

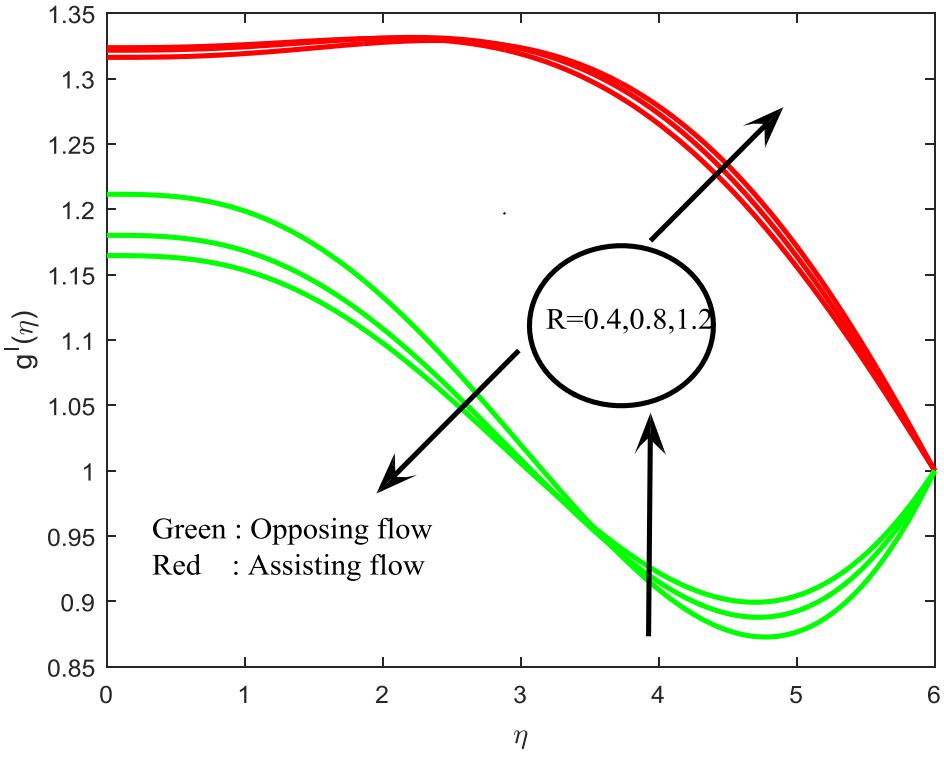

Figure 19. Induced Profiles for Different Values of Radiation Parameter

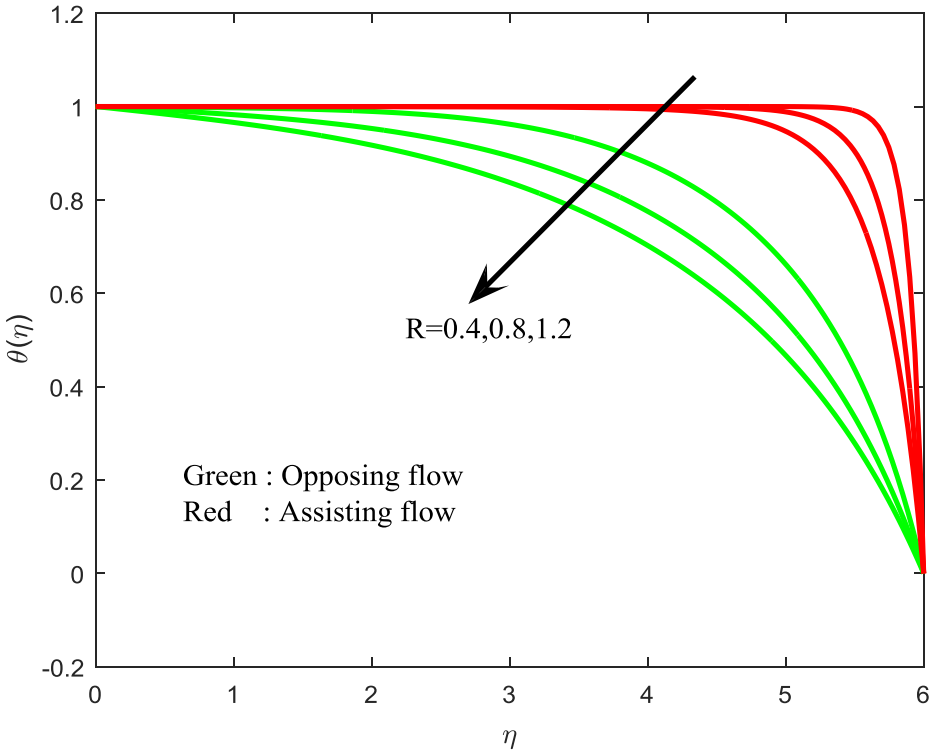

Figure 20. Temperature Profiles for Different Values of Radiation Parameter

4. Conclusions

The conclusions of the present study are as follows:

- The magnetic field parameter help to encourage the velocity, induced velocity profiles when $a / c = 3$. Whereas the velocity, induced velocity profiles are depreciated when $a / c = 0.5$.
- The skin friction coefficient is very less on opposing flows when compared with the assisting fluid flow over a cone.
- Dual behavior exists only for certain rage of a / c
- The induced magnetic field parameter improves the flow velocity and controls the heat transfer rate.
- The buoyancy parameter helps to improve the heat transfer rate for opposing flow and depreciates the same in assisting flow case.
- The chemical reaction parameter encourages the mass transfer rate as well as friction factor coefficient.

References

[1] W. L. Wilkinson, "Non-Newtonian fluids", Pergamon, New York, **(1960).**
[2] R. B. Bird, W. E. Stewart, E. N. Lightfoot, "Transport Phenomena", Wiley, New York, **(1960),** pp. 94-95.
[3] W. P. Walwander, T. Y. Chen, D. F. Cala, "An approximate Casson fluid model for tube flow of blood, Bio-rheology", vol. 12, **(1975),** pp. 111-119.
[4] D. D. Joye, "Shear rate and viscosity corrections for a Casson fluid in cylindrical (Couette) geometries", Journal of Colloid and Interface Sci., vol. 267, **(2003),** pp. 204-210.
[5] V. C. Kelessidis, R. Maglione, "Modeling rheological behavior of bentonite suspensions as Casson and Robertson-stiff fluids using Newtonian and true shear rates in Couette viscometer", Powder Technology, vol. 168, **(2006),** pp. 134-147.

[6] N. Sandeep, "Radiation and inclined magneticfield effects on unsteady hydromagnetic free convection flow past an impulsively moving vertical plate in porous medium", J. Applied and Fluid Mechanics, vol. 7, no. 2, **(2014)**, pp. 275-286.
[7] S. A. Shehzad, A. Alsaedi, T. Hayat, "Influence of thermophoresis and joule heating on the radiative flow of Jeffrey fluid with mixed convection", Brazilian J. Chemical Eng., vol. 30, no. 4**, (2013),** pp. 897-908.
[8] C. S. K. Raju, N. Sandeep, V. Sugunamma, M. Jayachandrababu, J. V. Ramanareddy, "Heat and mass transfer in magneto hydrodynamic Casson fluid over an exponentially permeable stretching surface", Eng. Sci. and Tech., an Int. J., **(2015)** http://dx.doi.org/10.1016/j.jestch.2015.05.010.
[9] M. M. Nandeppanavar, M. Subhas Abel, J. Tawade, "Heat transfer in a Walter's liquid B fluid over an impermeable stretching sheet with non-uniform heat source/sink and elastic deformation", J. Communications in Nonlinear Science and Numerical Simulation, vol. 15, no. 7, **(2010)**, pp. 1791-1802.
[10] T. Hayat, S. A. Shehzad, A. Alsaedi, M. S. Alhothuali, "Three-dimensional flow of Oldroyd-B fluid over surface with convective boundary conditions", Applied mathematics and mechanics, vol. 34, no. 4, **(2013)**, pp. 489-500.
[11] R. G. Hering, R. J. Grosh, "Laminar combined convection from a rotating cone", ASME J. Heat Transfer, vol. 85, **(1963),** pp. 29-34.
[12] D. Anilkumar, S. Roy, "Unsteady mixed convection flow on a rotating cone in a rotating fluid", Appl. Math. Computation, vol. 155, **(1963)**, pp. 545-561.
[13] S. Nadeem, S. Saleem, "Analytical treatment of unsteady mixed convection MHD flow on a rotating frame", J. Taiwan Institute of Chemical Engineers, vol. 44, no. 4, **(2013)**, pp. 596-604.
[14] C. S. K. Raju, M. Jayachandrababu, N. Sandeep, "Chemically reacting raidiative MHD Jeffery nanofluid flow over a cone in porous medium", Int. J. Eng. Res. In Africa, vol. 19, **(2016)**, pp. 75-90.
[15] S. Nadeem, S. Saleem, "Analytical study of rotating non-Newtonian nanofluid on a rotating cone", J. Thermo physics and Heat Transfer, vol. 28, no. 2, **(2014)**, pp. 295-302.
[16] S. Ahmad, N. M. Arifin, R. Nazar, I. Pop, "Mixed convection boundary layer flow along vertical thin needles: Assisting and Opposing flows", Int. Communications in Heat and Mass Transfer, vol. 35, **(2008)**, pp. 157-162.
[17] S. V. Subhashini, N. Samuel, I. Pop, "Effects of buoyancy assisting and opposing flows on mixed convection boundary layer flow over a permeable vertical surface", Int. Comm. Heat and Mass Transfer, vol. 38, **(2011)**, pp. 499-503.
[18] M. Jayachandrababu, N. Sandeep, C. S. K. Raju, "Heat and mass transfer in MHD Eyring-Powell nanofluid flow due to cone in porous medium", Int. J. Eng. Res. In Africa, vol. 19, **(2016)**, pp. 57-74.
[19] F. O. Patrulescu, T. Groshon, I. Pop, "Mixed convection boundary layer flow from a vertical truncated cone in nanofluid", Int. J. of Numerical Methods for Heat & Fluid Flow, vol. 24, no. 5, **(2014)**, pp. 1175-1190.
[20] C. S. K. Raju, N. Sandeep, C. Sulochana, V. Sugunamma, "Effects of aligned magnetic field and radiation on the flow of ferrofluids over a flat plate with non-uniform heat source/sink", Int. J. Sci. Eng., vol. 8, no. 2, **(2015)**, pp. 151-158.
[21] A. Ishak, R. Nazar, N. M. Arfin, I. Pop, "Dual solutions in mixed convection flow near a stagnation point on a vertical porous plate", Int. J. Thermal Sciences, vol. 47, **(2008)**, pp. 417-422.
[22] S. Saleem, S. Nadeem, R. UI Haq, "Buoyancy and metallic particle effects on an unsteady water-based fluid flow along a vertically rotating cone", Eur. Phys. J. Plus, vol. 129, **(2014)**, pp. 213.
[23] A. Ishak, R. Nazar, I. Pop, "Mixed convection stagnation point flow of a micropolar fluid towards a stretching sheet", Meccanica, vol. 43, **(2008)**, pp. 411-418.
[24] T. Hayat, B. Ashraf, S. A. Shehzad, E. Abouelmagd, "Three-dimensional flow of Eyring Powell nanofluid over an exponentially Stretching sheet", Int. J. Numerical Methods for Heat & Fluid Flow, vol. 25, no. 3, **(2015)**, pp. 593-616.
[25] M. Jayachandrababu, N. Sandeep, C. S. K. Raju, J. V. Ramanareddy, V. Sugunamma, "Nonlinear thermal radiation and induced magnetic field effects on stagnation point flow of ferrofluids", J. Advanced Physics, vol. 5, **(2015)**, pp. 1-7, Doi:10.1166/jap.2015.1271.
[26] F. M. Ali, R. Nazar, N. M. Arfin, I. Pop, "MHD stagnation point flow and heat transfer towards stretching sheet with induced magnetic field", Appl. Math. Mech. –Engl. Ed., vol. 32, no. 4, **(2011)**, pp. 409-418.
[27] N. Sandeep, C. Sulochana, "Dual solutions for unsteady mixed convection flow of MHD Micropolar fluid over a stretching/shrinking sheet with non-uniform heat source/sink", Engineering Science and Technology, an International Journal, vol. 18**, (2015),** pp. 738-745.
[28] N.Sandeep**,** A.Vijaya Bhaskar Reddy and V Sugunamma, "Effect of Radiation and Chemical Reaction on Transient MHD Free Convective flow over a Vertical Plate Through Porous Media", Chemical and Process Engineering Research 2**, (2012),** pp.1-9.
[29] C.S.K.Raju, N.Sandeep, "Heat and Mass Transfer in 3D non-Newtonian nano and Ferro fluids over a bidirectional stretching surface", Int.J.Eng. Research in Afrika, 21, **(2016)**, pp.33-51.
[30] C.Sulochana, S.P.Samrat, N.Sandeep, "Non-uniform heat source or sink effect on the flow of 3D Casson fluid in the presence of Soret and thermal radiation", Int.J.Eng. Resaech in Afrika, 20, **(2016),** pp.112-129.

Authors

C. S. K. Raju, obtained his M.Sc degree from Sri Venkateswara University, Tirupati in 2012. He presented papers in national and international conference and participated in national level workshops. At present he is doing his Ph.D in Fluid Dynamic Division, School of Advanced Sciences, VIT University, Vellore. His area of interest is Fluid Mechanics.

Dr. N. Sandeep, obtained his M.Sc degree from Sri Venkateswara University, Tirupati, India in 2006, M.Phil degree from Madurai Kamaraj University, Madurai in 2008 and Ph.D degree from Sri Venkateswara University, Tirupati in 2013. He published more than 90 papers in reputed scientific journals and presented several papers in national and international conferences. His area of interest is Fluid Mechanics.